crystals

MDPI

Article

Photoelastic Properties of Trigonal Crystals

Bohdan Mytsyk [1,*], Nataliya Demyanyshyn [1], Anatoliy Andrushchak [2] and Oleh Buryy [3]

[1] Optical Department, Karpenko Physico-Mechanical Institute of NAS of Ukraine, Naukova str. 5, 79060 Lviv, Ukraine; nmdem@ipm.lviv.ua
[2] Department of Applied Physics and Nanomaterials Science, Lviv Polytechnic National University, Bandery str. 12, 79013 Lviv, Ukraine; anatolii.s.andrushchak@lpnu.ua
[3] Department of Semiconductor Electronics, Lviv Polytechnic National University, Bandery str. 12, 79013 Lviv, Ukraine; oleh.a.buryi@lpnu.ua
* Correspondence: mytsyk@ipm.lviv.ua

Abstract: All possible experimental geometries of the piezo-optic effect in crystals of trigonal symmetry are studied in detail through the interferometric technique, and the corresponding expressions for the calculation of piezo-optic coefficients (POCs) π_{im} and some sums of π_{im} based on experimental data obtained from the samples of direct and $X/45°$-cuts are given. The reliability of the values of POCs is proven by the convergence of π_{im} obtained from different experimental geometries as well as by the convergence of some sums of POCs. Because both the signs and the absolute values of POCs π_{14} and π_{41} are defined by the choice of the right crystal-physics coordinate system, we here use the system whereby the condition $S_{14} > 0$ is fulfilled (S_{14} is an elastic compliance coefficient). The absolute value and the sign of S_{14} are determined by piezo-optic interferometric method from two experimental geometries. The errors of POCs are calculated as mean square values of the errors of the half-wave stresses and the elastic term. All components of the matrix of elasto-optic coefficients p_{in} are calculated based on POCs and elastic stiffness coefficients. The technique is tested on $LiTaO_3$ crystal. The obtained results are compared with the corresponding data for trigonal $LiNbO_3$ and $Ca_3TaGa_3Si_2O_{14}$ crystals.

Keywords: piezo-optic effect; elasto-optic effect; interferometric method; lithium tantalate; lithium niobate; catangasite

check for updates

Citation: Mytsyk, B.; Demyanyshyn, N.; Andrushchak, A.; Buryy, O. Photoelastic Properties of Trigonal Crystals. *Crystals* **2021**, *11*, 1095. https://doi.org/10.3390/cryst11091095

Academic Editor: Daniele Rinaldi

Received: 16 August 2021
Accepted: 3 September 2021
Published: 8 September 2021

1. Introduction

According to the terminology adopted here, low-symmetry elasto-optic materials are the ones which, in addition to principal components of the tensor of elasto-optic coefficients (ELOCs) p_{in} (indices i, n = 1, 2, 3), have non-principal non-diagonal components, expressed as p_{in}, where i, n = 4, 5, 6. In particular, calcium tungstate $CaWO_4$ (crystal class $4/m$) has 10 independent components p_{in} [1,2], including the non-principal non-diagonal components p_{16}, p_{61}, p_{45}, lithium niobate $LiNbO_3$ (class $3m$) and lithium tantalate $LiTaO_3$ (class $3m$) investigated in this paper, as well as independent components of calcium-tantalum gallosilicate $Ca_3TaGa_3Si_2O_{14}$ (class 32)–8, including two non-principal problematic coefficients p_{14} and p_{41}, etc. The mentioned non-principal coefficients are identified as 'problematic' because of the ambiguity involved in their determination. To address this ambiguity, in terms of both signs and absolute values, the positive directions of axes of the right crystal-physics coordinate system should be explicitly chosen (see, e.g., [3,4] for details).

Let us point out the reasons for the complexity of the determination of all matrix components p_{in} and their signs. As it is known, the acousto-optic figure-of-merit M_2 can be found using the Dixon–Cohen method [5,6] based on the expression:

$$M_2 = \frac{n_i^6 p_{in}^2}{\rho V_n^3}, \qquad (1)$$

where n_i is a refractive index of a crystal, ρ is its density, and V_n is an acoustic wave velocity.

However, the coefficient p_{in} appears in Equation (1) in the second power, so the determination of the sign of p_{in} is impossible. Moreover, for the complex geometry of the experiment, when not one p_{in} coefficient, but rather the sum of p_{in} coefficients, is included in Equation (1) (among them, the ones with the indices i, n equal to 4, 5, 6), it is also difficult to determine the absolute values of p_{in}. It should be mentioned that the expressions for the determination of particular coefficients p_{in} are absent in [5,6], but the correctness of this method is not doubted, because the values of ELOCs p_{in} defined in these papers for two dozen of acousto-optic crystals were further confirmed by other authors and, in particular, by other methods. However, the signs of ELOCs were found only for the simplest case of high-symmetry cubic crystals.

The acousto-optic methods of Bergmann-Fues [7] and Pettersen [8] make it possible to determine only the p_{12}/p_{11} relation or the complex combinations of p_{in} coefficients, such as $(p_{11} + p_{12} + 2p_{44})/(p_{11} + p_{12} - 2p_{44})$, for cubic crystals. The analogous expressions for the crystals of lower symmetry were not given. The diffraction method of Narasimhamurty [2,9] is useful only for the determination of the combinations of ELOCs, such as $p_{33}n_3^3/p_{13}n_1^3$, in trigonal crystals (crystal classes 32, 3m). The Brillouin scattering method makes it possible to define the p_{in} coefficients for cubic crystals [10,11], or only the principal components of the p_{in} matrix (i, n = 1, 2, 3), for crystals of lower symmetry (the results for three principal ELOCs of tetragonal crystals are given in [12]). All p_{in} coefficients (including their signs) for $LiNbO_3$ (symmetry class 3m) and $CaMoO_4$ (class 4/m) were determined using this method in [13,14]. However, because of the absence of the expressions for ELOCs in these papers, their results cannot be used for the complete study of the elasto-optic effect in low-symmetry crystals. It should be emphasized that the values of the p_{in} coefficients in the modeling of lithium niobate crystal, as determined by acousto-optic methods, are essentially different according to data provided by different authors: by 1.3–1.5 times for elasto-optic coefficients p_{12}, p_{31}, p_{41} and by 1.6–2.1 times for p_{11}, p_{13}, p_{14}, p_{33}, p_{44} [13,15]. Thus, the errors in the determination of ELOCs are high. The acousto-optic techniques used for the determination of different combinations of ELOCs are described in [2,16].

Therefore, only the use of acousto-optic methods prevents the determination of the values and signs of all components of the ELOC matrix with high precision, especially for the crystals in p_{in} matrices that contain such problematic coefficients as p_{14}, p_{41}, p_{25}, p_{52}, p_{16}, p_{61}, p_{64}, p_{45}, etc. In particular, the absolute values and signs of ELOCs for orthorhombic crystals characterized by the rather simple p_{in} matrix (without problematic coefficients) were completely determined in [17,18] using three methods (acousto-optic, interferometric and polarization-optical methods) including the application, in addition to uniaxial pressure, of the hydrostatic method to the samples.

Here, the matrix of p_{in} coefficients for trigonal lithium tantalate crystals $LiTaO_3$ (symmetry class 3m) was filled based on the experimentally determined matrix of piezo-optic coefficients (POCs) π_{im} and the known tensor expression

$$p_{in} = \pi_{im}C_{mn}, \quad (2)$$

where C_{mn} are elastic stiffness coefficients.

The coefficients π_{im} were determined by means of the static interferometric method described in papers [2–4,19–23]. These papers were focused on the reliability (objectivity) of the obtained results. For this purpose, the maximal number of the experimental geometries was considered and used, the corresponding expressions were written and the specific values of POCs π_{im} and the sums of POCs, such as $\pi_{12} + \pi_{13}$, $\pi_{24} + 2\pi_{42} = -(\pi_{14} + 2\pi_{41})$, etc., obtained from different experimental geometries, were compared (particularly, the π_{11} coefficient is determined from six experimental geometries). The main results of the investigations of the photoelasticity (piezo- and elasto-optic effects) of lithium tantalate $LiTaO_3$ were compared with the results for trigonal lithium niobate $LiNbO_3$ and catangasite $Ca_3TaGa_3Si_2O_{14}$ crystals.

It should be noted that the polarization-optical (see, e.g., [16–18,24–27]) and conoscopic [28–33] methods are sometimes used for investigations of crystal photoelasticity. However, in this paper, the photoelasticity of lithium tantalate is solely studied using the interferometric technique.

2. Theory: Main Results

Lithium tantalate ($LiTaO_3$) crystals belong to $3m$ symmetry class [15] and their matrices of piezo- and elasto-optic coefficients (π_{im} and p_{ik}) include eight independent non-zero components [1,2] (Figure 1).

$$[\pi_{im}]=\begin{pmatrix} \pi_{11} & \pi_{12} & \pi_{13} & \pi_{14} & 0 & 0 \\ \pi_{12} & \pi_{11} & \pi_{13} & -\pi_{14} & 0 & 0 \\ \pi_{31} & \pi_{31} & \pi_{33} & 0 & 0 & 0 \\ \pi_{41} & -\pi_{41} & 0 & \pi_{44} & 0 & 0 \\ 0 & 0 & 0 & 0 & \pi_{44} & 2\pi_{41} \\ 0 & 0 & 0 & 0 & \pi_{14} & \pi_{66} \end{pmatrix} \qquad [p_{ik}]=\begin{pmatrix} p_{11} & p_{12} & p_{13} & p_{14} & 0 & 0 \\ p_{12} & p_{11} & p_{13} & -p_{14} & 0 & 0 \\ p_{31} & p_{31} & p_{33} & 0 & 0 & 0 \\ p_{41} & -p_{41} & 0 & p_{44} & 0 & 0 \\ 0 & 0 & 0 & 0 & p_{44} & p_{41} \\ 0 & 0 & 0 & 0 & p_{14} & p_{66} \end{pmatrix}$$

Figure 1. The matrices of piezo- and elasto-optic coefficients of trigonal crystal classes 32, $3m$ and $\bar{3}m$ (π_{66} = $\pi_{11} - \pi_{12}$; p_{66} = $(p_{11} - p_{12})/2$).

Five independent principal piezo-optic coefficients (POCs) π_{11}, π_{12}, π_{13}, π_{31} and π_{33} are determined on the sample of direct cuts (Figure 2a) using simple formulae for their calculation on the basis of experimental data (see below). The main difficulties in filling of POC and ELOC matrices relate to the determination of three non-principal POCs—π_{14}, π_{41} and π_{44}. The piezo-optic effect (POE) should, to this end, be investigated on the sample of the $X/45°$ cut. In addition to non-principal POCs, the principal POC π_{11} as well as the sums of principal POCs such as π_{21} + π_{31}, π_{12} + π_{13}, π_{22} + π_{23}, etc. can be determined on this sample. Comparison of these sums of POC with the analogous ones for principal coefficients π_{im} determined on the direct cut sample makes it possible to confirm the reliability of the POC values as well as piezo-optical identity of the samples cut from the different parts of crystal boule or from different boules.

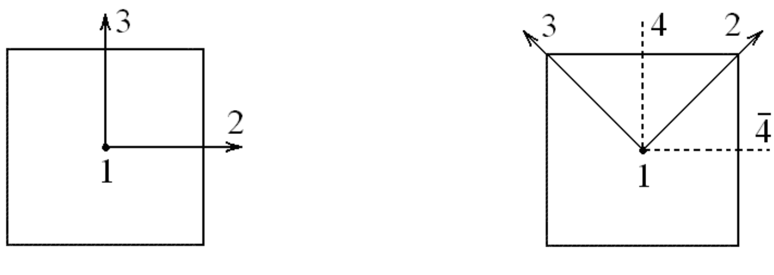

(**a**) (**b**)

Figure 2. The schemes of samples for investigation of piezo-optic effect in $LiTaO_3$ crystal: (**a**) the sample of direct cuts, (**b**) the sample of the $X/45°$-cut. The directions 1, 2, 3 correspond to the axes of the optical indicatrix X, Y, Z.

For the determination of POC π_{im} using the interferometric method, the change of the optical path must be calculated [3] as:

$$\delta\Delta_k = \delta(n_i \cdot d_k) = \delta n_i \cdot d_k + \delta d_k(n_i - 1), \tag{3}$$

where n_i is a refractive index of the crystal and d_k is the crystal thickness in the direction of light propagation.

After substituting the known expressions for the change of the refractive index δn_i under the influence of the mechanical stress σ_m and for the deformation of the sample δd_k along the direction of light propagation, it is easy to obtain the expression for $\delta\Delta_k$, which contains POCs, represented by π_{im}, and elastic compliance coefficients, expressed as S_{km} (see, e.g., [3,20]):

$$\delta\Delta_k = -\frac{1}{2}\pi_{im}\sigma_m d_k n_i^3 + S_{km}\sigma_m d_k(n_i - 1). \tag{4}$$

For the known method of half-wave stresses (when $\delta\Delta_k = \lambda/2$ and $\sigma_m = \sigma_{im}$ is a half-wave mechanical stress), Expression (4) transforms to:

$$\pi_{im} = -\frac{\lambda}{n_i^3\sigma_{im}d_k} + 2S_{km}\frac{(n_i-1)}{n_i^3} = -\frac{\lambda}{n_i^3\sigma_{im}^o} + 2S_{km}\frac{(n_i-1)}{n_i^3}; \tag{5}$$

where $\sigma_{im}^o = \sigma_{im} \cdot d_k$ is so called control stress, which is a characteristic of the material; despite the half-wave stress σ_{im}, which is a characteristic of a sample depended on its dimensions, the indices k, i and m correspondingly designate the directions of light propagation, polarization and the application of uniaxial pressure σ_m, and λ is the light wavelength.

Let us consider the examples of the specific expressions for the determination of the principal POCs based on Formula (2). In particular, under the experimental conditions $k = 3$ (the direction of light propagation), $i = 1$ (the direction of light polarization), $m = 1$ or $m = 2$ (directions of the application of uniaxial pressure σ_1 or σ_2), for the principal POCs π_{11} and π_{12}, we obtain the following expressions for the experimental conditions (5):

$$\pi_{11} = -\frac{\lambda}{n_1^3\sigma_{11}^o} + \frac{2S_{13}}{n_1^3}(n_1 - 1); \pi_{12} = -\frac{\lambda}{n_1^3\sigma_{12}^o} + \frac{2S_{23}}{n_1^3}(n_1 - 1), \tag{6}$$

where it is taken into account that the matrix of elastic compliance coefficients is symmetrical ($S_{km} = S_{mk}$), so $S_{31} = S_{13}$, $S_{32} = S_{23}$.

Expression (5) is valid for the determination of principal POCs π_{im} (i, m = 1, 2, 3) on the direct cut sample (Figure 2a), the edges of which are perpendicular to the crystal-physics axes X, Y, Z (the axes of the optical indicatrix). Such expressions are significantly complicated in the case of the investigation of POE on the sample of $X/45°$-cut (Figure 2b). For example, for the experimental conditions $m = 4$, $k = \bar{4}$, $i = 1$ (Figure 2b), the following expression is written for the determination of POC π_{14} in [3]:

$$\delta\Delta_{\bar{4}} = -\frac{\pi_{12} + \pi_{13} + \pi_{14}}{4}\sigma d_{\bar{4}} n_1^3 + \frac{1}{4}(S_{11} + 2S_{13} + S_{33} - S_{44})\sigma d_{\bar{4}}(n_1 - 1), \tag{7}$$

and the analogous one for the symmetrical experimental conditions ($m = \bar{4}$, $k = 4$, $i = 1$):

$$\delta\Delta_4 = -\frac{\pi_{12} + \pi_{13} - \pi_{14}}{4}\sigma d_4 n_1^3 + \frac{1}{4}(S_{11} + 2S_{13} + S_{33} - S_{44})\sigma d_4(n_1 - 1), \tag{8}$$

where σ is a value of the uniaxial pressure.

In the case of the half-wave method ($\delta\Delta_4 = \delta\Delta_{\bar{4}} = \lambda/2$, $\sigma = \sigma_{im} = \sigma_{14}$ and $\sigma = \sigma_{im} = \sigma_{1\bar{4}}$), these expressions make it possible to obtain two equations for the determination of POC π_{14}:

$$\pi_{12} + \pi_{13} + \pi_{14} = -\frac{2\lambda}{n_1^3\sigma_{14}d_{\bar{4}}} + (S_{11} + 2S_{13} + S_{33} - S_{44})\frac{(n_1-1)}{n_1^3}, \tag{9}$$

$$\pi_{12} + \pi_{13} - \pi_{14} = -\frac{2\lambda}{n_1^3\sigma_{1\bar{4}}d_4} + (S_{11} + 2S_{13} + S_{33} - S_{44})\frac{(n_1-1)}{n_1^3}. \tag{10}$$

These two equations are reduced to one (T. 6) in Table 1, where the products $\sigma_{14}d_{\bar{4}}$ and $\sigma_{1\bar{4}}d_4$ are substituted by the symbols σ_{14}^o and $\sigma_{1\bar{4}}^o$, thus designating the control stresses for the above-mentioned direct and symmetrical experimental conditions.

Table 1. The expressions for the determination of POCs π_{im} on the sample of $X/45°$-cut for crystal classes 32, $3m$ and $\bar{3}\,m$ given for the method of half-wave (control) stresses.

Experimental Conditions	Expressions	
	Sample of $X/45°$-Cut	
$m = 1$ $k = 4(\bar{4})$ $i = 1$	$\pi_{11} = -\frac{\lambda}{n_1^3\sigma^o_{11\ \mid\ k=4(\bar{4})}} + (S_{12} + S_{13} \pm S_{14})\frac{n_1-1}{n_1^3}$	T. 1
	$\pi_{11} = -\frac{\lambda}{2n_1^3}\left(\frac{1}{\sigma^o_{11\ \mid\ k=4}} + \frac{1}{\sigma^o_{11\mid k=\bar{4}}}\right) + (S_{12} + S_{13})\frac{n_1-1}{n_1^3}$	T. 2
$m = 1$ $k = 4(\bar{4})$ $i = \bar{4}(4)$	$\pi_{21} + \pi_{31} \mp 2\pi_{41} = -\frac{2\lambda}{n_4^3\sigma^o_{\bar{4}1(41)}} + 2(S_{12} + S_{13} \pm S_{14})\frac{n_4-1}{n_4^3}$	T. 3
	$\pi_{41} = -\frac{\lambda}{2n_4^3}\left(\frac{1}{\sigma^o_{41}} - \frac{1}{\sigma^o_{\bar{4}1}}\right) - S_{14}\frac{n_4-1}{n_4^3}$	T. 4
	$\pi_{21} + \pi_{31} = -\frac{\lambda}{n_4^3}\left(\frac{1}{\sigma^o_{41}} + \frac{1}{\sigma^o_{\bar{4}1}}\right) + 2(S_{12} + S_{13})\frac{n_4-1}{n_4^3}$	T. 5
$m = 4(\bar{4})$ $k = \bar{4}(4)$ $i = 1$	$\pi_{12} + \pi_{13} \pm \pi_{14} = -\frac{2\lambda}{n_1^3\sigma^o_{14(1\bar{4})}} + (S_{11} + 2S_{13} + S_{33} - S_{44})\frac{n_1-1}{n_1^3}$	T. 6
	$\pi_{14} = -\frac{\lambda}{n_1^3}\left(\frac{1}{\sigma^o_{14}} - \frac{1}{\sigma^o_{1\bar{4}}}\right)$	T. 7
	$\pi_{12} + \pi_{13} = -\frac{\lambda}{n_1^3}\left(\frac{1}{\sigma^o_{14}} + \frac{1}{\sigma^o_{1\bar{4}}}\right) + (S_{11} + 2S_{13} + S_{33} - S_{44})\frac{n_1-1}{n_1^3}$	T. 8
$m = 4(\bar{4})$ $k = \bar{4}(4)$ $i = 4(\bar{4})$	$\pi_{22} + \pi_{23} \pm \pi_{24} + \pi_{32} + \pi_{33} \pm 2\pi_{42} + 2\pi_{44} =$ $= -\frac{4\lambda}{n_4^3\sigma^o_{44(\bar{4}\bar{4})}} + 2(S_{11} + 2S_{13} + S_{33} - S_{44})\frac{n_4-1}{n_4^3}$	T. 9
	$\pi_{22} + \pi_{23} + \pi_{32} + \pi_{33} + 2\pi_{44} =$ $= -\frac{2\lambda}{n_4^3}\left(\frac{1}{\sigma^o_{44}} + \frac{1}{\sigma^o_{\bar{4}\bar{4}}}\right) + 2(S_{11} + 2S_{13} + S_{33} - S_{44})\frac{n_4-1}{n_4^3}$	T. 10
	$\pi_{24} + 2\pi_{42} = -\frac{2\lambda}{n_4^3}\left(\frac{1}{\sigma^o_{44}} - \frac{1}{\sigma^o_{\overline{44}}}\right)$	T. 11
$m = 4(\bar{4})$ $k = 1,$ $i = 2$	$\pi_{22} + \pi_{23} \pm \pi_{24} = -\frac{2\lambda}{n_1^3\sigma^o_{24(2\bar{4})}} + 2(S_{12} + S_{13} \pm S_{14})\frac{n_1-1}{n_1^3}$	T. 12
	$\pi_{24} = -\frac{\lambda}{n_1^3}\left(\frac{1}{\sigma^o_{24}} - \frac{1}{\sigma^o_{2\bar{4}}}\right) + 2S_{14}\frac{n_1-1}{n_1^3}$	T. 13
	$\pi_{22} + \pi_{23} = -\frac{\lambda}{n_1^3}\left(\frac{1}{\sigma^o_{24}} + \frac{1}{\sigma^o_{2\bar{4}}}\right) + 2(S_{12} + S_{13})\frac{n_1-1}{n_1^3}$	T. 14
$m = 4(\bar{4})$ $k = 1$ $i = 3$	$\pi_{32} + \pi_{33} = -\frac{2\lambda}{n_3^3\sigma^o_{34(3\bar{4})}} + 2(S_{12} + S_{13} \pm S_{14})\frac{n_3-1}{n_3^3}$	T. 15
	$\pi_{32} + \pi_{33} = -\frac{\lambda}{n_3^3}\left(\frac{1}{\sigma^o_{34}} + \frac{1}{\sigma^o_{3\bar{4}}}\right) + 2(S_{12} + S_{13})\frac{n_3-1}{n_3^3}$	T. 16

Note: the symmetry conditions of the experiment are indicated in brackets, e.g., in Equation (T. 6), the control stresses are written in the form of $\sigma^o_{14(1\bar{4})}$, i.e., σ^o_{14} corresponds to the sign (+) at π_{14}, $\sigma^o_{1\bar{4}}$ –to the sign (−), etc.

Because the signs before the coefficient π_{14} are opposite in Equations (9) and (10), after their subtraction, one can dispose of the principal POCs π_{12} and π_{13}, as well as the elastic item:

$$\pi_{14} = -\frac{\lambda}{n_1^3}\left(\frac{1}{\sigma^o_{14}} - \frac{1}{\sigma^o_{1\bar{4}}}\right), \tag{11}$$

whereas, after the summation of (9) and (10), one can obtain the expression for the calculation of the sum π_{12} + π_{13} based on the same control stresses:

$$\pi_{12} + \pi_{13} = -\frac{\lambda}{n_1^3}\left(\frac{1}{\sigma^o_{14}} + \frac{1}{\sigma^o_{1\bar{4}}}\right) + (S_{11} + 2S_{13} + S_{33} - S_{44})\frac{n_1 - 1}{n_1^3} \tag{12}$$

This sum of POCs will make it possible to confirm the reliability of the values of principal POCs π_{12} and π_{13}, the objectivity of the experimentally determined control stressesσ^o_{14}, $\sigma^o_{1\bar{4}}$ and, correspondingly, the reliability of the value of POC π_{14}.

All other relationships for the calculation of the non-principal POCs and different variants of sums of principal POCs based on the experimental values of the control stresses σ^o_{im} are given in Table 1. The experimental geometries for the determination of the principal

POC π_{11} on the sample of $X/45°$-cut are also considered, see formulae (T. 1), (T. 2) in Table 1. The expression for the determination of POC π_{44} (T. 9) is particularly complex; it includes the complex sums of POCs and elastic compliance coefficients S_{km}. However, after the summation or subtraction of expressions that differ in terms of sign at some non-principal POCs, simpler expressions can be obtained for direct and symmetrical experimental conditions. In particular, the problematic POCs $\pi_{24} = -\pi_{14}$ and $2\pi_{42} = -2\pi_{41}$ are absent in the expression (T. 10) and all principal POCs and POC π_{44} as well as all elastic compliance coefficients S_{km} are absent in (T. 11). Accordingly, the absolute errors of the determination of corresponding non-principal POCs will be significantly lower.

3. The Experimental Technique

The investigated $LiTaO_3$ crystals were grown at the SRC 'Electron-Carat' (Lviv, Ukraine) by means of the Czochralski technique from the congruent melt. The monodomainization of the crystals was carried out by heating them to a temperature that was between 30 and 40 degrees higher than the Curie point, subsequent connection to the dc voltage source (10–15 V), and slow cooling to room temperature.

As mentioned above, lithium tantalate crystals belong to the symmetry class $3m$. The matrix of POCs correspondingly includes 8 independent components π_{im}. For their determination, the samples of the direct cut (Figure 2a) and $X/45°$-cut (Figure 2b), with the dimensions of about 7 mm × 7 mm × 7 mm, were investigated. The samples withstood high mechanical stress of about 300 kg/cm^2. The interferometric technique was used for the determination of absolute POCs π_{im}. The experimental set-up was based on the one-pass Mach–Zehnder laser interferometer, and the sample was placed in one of the interferometer shoulders (see, e.g., [3,21]). For the determination of sign of the optical path change $\delta\Delta_k$, which was induced by uniaxial pressure, a thin plate of fused silica was placed in the measuring shoulder of the interferometer after the sample. The rotation of the plate from the direction perpendicular to the direction of light beam propagation increased the optical path of the light beam and, correspondingly, led to the displacement of the interferometric band in a certain direction. If under the influence of the uniaxial pressure σ_m, the bands shifted to the same direction, and the sign of $\delta\Delta_k$ was positive, whereas in the opposite direction, it was negative. This sign was placed before λ in the formulae for the calculation of POCs π_{im} on the basis of control stresses σ^o_{im} and, moreover, it had to be taken into account that the stresses of compression were attributed to the "minus" sign. A detailed description of the experimental set-up and the procedure of POCs determination was given in paper [21].

Let us recall that in the case of complex POC matrix containing such non-principal components as π_{14}, π_{41}, etc., the ambiguity of the determination of these POCs both on signs and absolute values (see, e.g., [3]) exists depending on the choice of the positive signs of the right coordinate system X, Y, Z. Usually, the signs of the axes are chosen on the basis of piezo-electric effect [3,4,27]. However, the piezo-electric coefficients d_{lm} of lithium tantalate are relatively low (2–3 times lower than the ones of lithium niobate [15]). Correspondingly, it was impossible to specify the signs of the right coordinate system axes X, Y and Z based on the d_{lm} coefficients. Therefore, in this case, the positive signs of the axes Y, Z and, correspondingly, the directions 4 and $\bar{4}$, were chosen on the basis of the positive value of the elastic compliance coefficient S_{14}.

The elastic compliance coefficient S_{14} of the crystals of 32, $3m$ and $\bar{3}m$ classes could be determined via the piezo-optic technique. Namely, if two equations (T. 1 in Table 1) (they differed according to the signs «+» or «–» before the S_{14} coefficient and the control stresses $\sigma^o_{11\,|\,k=4}$ and $\sigma^o_{11|k=\bar{4}}$) were added, the expression (T. 2) was obtained for the determination of π_{11} on the sample of $X/45°$-cut. If these Equations were subtracted, one obtained the expression for the determination of the S_{14} coefficient:

$$S_{14} = \frac{\lambda}{2(n_1 - 1)} \left(\frac{1}{\sigma^o_{11\,|\,k=4}} - \frac{1}{\sigma^o_{11\,|\,k=\bar{4}}} \right). \tag{13}$$

It should be noted that the values of control stresses $\sigma^o_{11\,|\,k=4}$ i $\sigma^o_{11|k=\bar{4}}$ traded places depending on the choice of coordinate system on the sample of the $X/45°$-cut (Figure 3). The elastic compliance coefficient S_{14} had the sign «+» or «–».

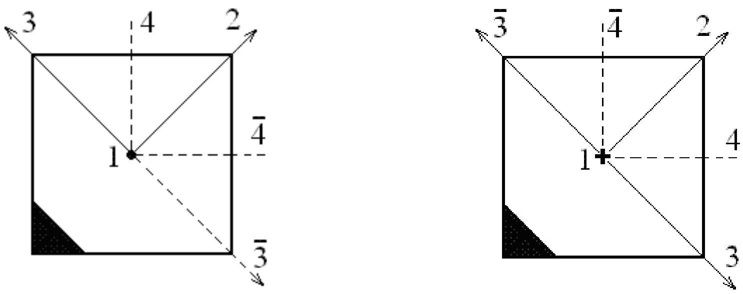

(**a**) (**b**)

Figure 3. The schemes of the choice of coordinate system on the sample of $X/45°$-cut: the system in figure (**b**) is obtained from the one in figure (**a**) by its rotation at the angle of 180° around axis 2.

If the uniaxial pressure was applied along the direction 1 (m = 1), we chose the direction of light polarization in the same direction (i = 1) and the direction of light propagation was ensured along 4 (Figure 3a), and thus, we obtained the control stress $\sigma^o_{11\,|\,k=4}$. If the other coordinate system was chosen on the same sample, such as the one in Figure 3b, the control stress had the designation $\sigma^o_{11|k=\bar{4}}$. Thus, the experimental value of the control stress needed to be placed in the position of the first item in brackets in expression (13) rather than in the position of the second item. Therefore, the S_{14} coefficient could be determined only to within the sign.

In this investigation, we chose the coordinate system (one of the systems shown in Figure 3) that corresponded to the condition $S_{14} > 0$. This condition was used because, in three papers [34–36], the coefficients S_{14} were commensurate with the values and were positive (see Table 2). This coordinate system was used for all studies of POE in $LiTaO_3$ crystals.

Table 2. Elastic stiffness coefficients C_{mk} (in 10^{11} N/m^2) and elastic compliance coefficients S_{km} (in 10^{-12} m^2/N) of $LiTaO_3$ crystals.

C_{mk}	C_{11}	C_{33}	C_{12}	C_{13}	C_{14}	C_{44}	Refer.
1.	2.39	2.84	0.41	0.80	−0.22	1.13	[34]
2.	2.38	2.82	0.21	0.73	−0.27	1.17	[35]
3.	2.421	2.752	0.375	0.827	−0.237	1.139	[36]
S_{km}	S_{11}	S_{33}	S_{12}	S_{13}	S_{14}	S_{44}	Refer.
4.	4.76	4.19	−0.5	−1.20	1.02	9.3	[34]
5.	4.68	4.14	−0.16	−1.17	1.10	9.00	[35]
* 6.	4.72	4.42	−0.37	−1.31	0.98	9.16	* Calculated

Note: the asterisk (*) designates the row where the values of S_{km} were calculated on the basis of the matrix of elastic shiftiness coefficients C_{mk} [36] using the inverse matrix method.

It should be emphasized that the value of the S_{14} coefficient could be defined by the piezo-optic interferometric technique for other experimental conditions, and this was used for the determination of the sum $\pi_{32} + \pi_{33}$, see formula (T.15) in Table 1. Through the summation of two Equations (T.15), one could obtain the expression (T. 16) for sum $\pi_{32} + \pi_{33}$, which could be used to prove the reliability of POC values $\pi_{31} = \pi_{32}$ and π_{33}. By means of the subtraction of Equations (T.15), which differ in terms of the sign before the S_{14} coefficient, we obtained one more equation for the determination of S_{14} (under other experimental conditions, on the sample of the $X/45°$-cut: $m = 4$ or $\bar{4}$, $k = 1$, $i = 3$) based on the control stresses σ^o_{34} and $\sigma^o_{3\bar{4}}$:

$$S_{14} = \frac{\lambda}{2(n_3 - 1)} \left(\frac{1}{\sigma^o_{34}} - \frac{1}{\sigma^o_{3\bar{4}}} \right). \tag{14}$$

The experimental values of the control stresses were $\sigma^o_{11\ |\ k=4}$ = −103 kG/cm and $\sigma^o_{11|k=\bar{4}}$ = −185 kG/cm; thus, it followed from (13) that S_{14} = + 1.18 ± 0.31 (in units, 10^{-12} m^2/N). From this point onwards, it was taken into account that the stresses of compressions had the sign '−'. On the other hand, if the experimental values of the control stresses σ^o_{34} = 450 kG/cm and $\sigma^o_{3\bar{4}}$ = 170 kG/cm were substituted in (14), one could obtain S_{14} = + 1.00 ± 0.17 (in units, 10^{-12} m^2/N). Thus, both values of S_{14} were commensurate with the limits of experimental errors. However, we used the second one (1.00 ± 0.17), because the error of this S_{14} coefficient was significantly lower. It should be noted that both values of the S_{14} coefficient coincided to a significant extent (within the limits of errors) with the values of S_{14} determined in papers [34–36] (see Table 2).

4. Results of Investigations of POE in $LiTaO_3$ Crystals and Their Analysis

For the calculation of absolute POCs of lithium tantalate, the experimentally defined control stresses, represented as σ^o_{im} (Table 3), and the refractive indices indicated in [15] ($n_1 = n_o$ = 2.175, $n_3 = n_e$ = 2.180 for T_{room} and the wavelength of λ = 632.8 nm) were used. The refractive indices along the diagonal directions 4 and $\bar{4}$ were determined in accordance with the known expression

$$n_4 = n_{\bar{4}} = \frac{\sqrt{2}}{\sqrt{a_2 + a_3}} = \sqrt{2} \Bigg/ \sqrt{\frac{1}{n_2^2} + \frac{1}{n_3^2}} = \frac{\sqrt{2} n_2 n_3}{\sqrt{n_2^2 + n_3^2}}, \tag{15}$$

where $a_i = 1/\ {n_i}^2$ is polarization constants.

Table 3. Results of investigations of POE in $LiTaO_3$ crystals (λ = 632.8 nm, T = 20 °C, 1 Br = 1 Brewster = 10^{-12} m^2/N).

No.	Experimental Conditions			σ^o_{im}, kG/cm	π_{im}, Br
	m	k	i		
			Direct cut samples, Figure 2a		
1	1	2	1	$\sigma^\circ_{11} = -104$	$\pi_{11} = -0.64 \pm 0.06$
2			3	$\sigma^\circ_{31} = 104$	$\pi_{31} = 0.56 \pm 0.06$
3	1	3	1	$\sigma^\circ_{11} = -175$	$\pi_{11} = -0.63 \pm 0.05$
4			2	$\sigma^\circ_{21} = 86$	$\pi_{21} = 0.46 \pm 0.07$
5	2	1	2	$\sigma^\circ_{22} = -110$	$\pi_{22} = -0.61 \pm 0.06$
6			3	$\sigma^\circ_{32} = 112$	$\pi_{32} = 0.52 \pm 0.06$
7	2	3	2	$\sigma^\circ_{22} = -180$	$\pi_{22} = -0.62 \pm 0.04$
8			1	$\sigma^\circ_{12} = 84$	$\pi_{12} = 0.48 \pm 0.08$
9	3	1	3	$\sigma^\circ_{33} = \infty$	$\pi_{33} = -0.27 \pm 0.01$
10			2	$\sigma^\circ_{23} = 65$	$\pi_{23} = 0.70 \pm 0.10$
11	3	2	3	$\sigma^\circ_{33} = \infty$	$\pi_{33} = -0.27 \pm 0.01$
12			1	$\sigma^\circ_{13} = 62.5$	$\pi_{13} = 0.74 \pm 0.10$
			Sample of X/45°-cut, Figure 2b		
13	1	4	1	$\sigma^\circ_{11} = -103$	$\pi_{11} = -0.63 \pm 0.04$
14			$\bar{4}$	$\sigma^o_{\bar{4}1} = 70$	$\pi_{41} = -0.29 \pm 0.05$
15	1	$\bar{4}$	1	$\sigma^\circ_{11} = -185$	$\pi_{11} = -0.63 \pm 0.04$
16			4	$\sigma^\circ_{41} = 200$	$\pi_{12} + \pi_{31} = 0.90 \pm 0.09$
17	4	1	2	$\sigma^\circ_{24} = 200$	$\pi_{24} = 0.43 \pm 0.04$
18			3	$\sigma^\circ_{34} = 450$	$\pi_{31} + \pi_{33} = 0.20 \pm 0.04$
19	4	$\bar{4}$	1	$\sigma^\circ_{14} = 130$	$\pi_{14} = -0.37 \pm 0.10$
20			4	$\sigma^\circ_{44} = 140$	$\pi_{44} = -0.06 \pm 0.09$
21	$\bar{4}$	1	2	$\sigma^o_{2\bar{4}} = 470$	$\pi_{11} + \pi_{13} = 0.14 \pm 0.04$
22			3	$\sigma^o_{3\bar{4}} = 170$	$\pi_{31} + \pi_{33} = 0.20 \pm 0.04$
23	$\bar{4}$	4	1	$\sigma^o_{1\bar{4}} = 74$	$\pi_{12} + \pi_{13} = 1.04 \pm 0.12$
24			$\bar{4}$	$\sigma^o_{\bar{4}\bar{4}} = -1250$	$\pi_{24} + 2\pi_{42} = 0.99 \pm 0.09$

Note: the sign 'minus' before the control stresses σ^o_{11}, σ^o_{22}, $\sigma^o_{\bar{4}\bar{4}}$ (rows 1, 3, 5, 24, etc.) indicates the shortening of the optical pass under the influence of the uniaxial pressure; when the values of π_{im} are calculated, this sign is placed before λ; at this point, it is taken into account that the stresses of compression have the sign 'minus'.

The elastic compliance coefficients S_{km} included in the expressions for the determination of POCs π_{im} are given in Table 2. The best convergence of π_{im} coefficient calculations (i.e., the closest values of specific POC π_{im} determined for different experimental geometries, or the same sums of POCs within the limits of the precision of their calculation found from direct measurements or formed from independent POCs π_{im}) was ensured when the elastic compliance coefficients from [35] was used, see row 5 in Table 2. The elastic shiftiness coefficients C_{mn} (row 2 in Table 2), for the calculations of ELOCs p_{in} (see Section 5), were taken from the same paper.

The calculations of the errors of POCs π_{im} were carried out on the basis of the experimental errors of control stresses σ^{o}_{im}, which were about 10% of the value of σ^{o}_{im}, and the errors of elastic compliance coefficients S_{km}, which were about 5% of the value of S_{km}, as was also the case in our other papers.

Comments to the Results of POE Investigations in $LiTaO_3$ Crystals

1. As can be seen in Table 3, the π_{11} coefficient was determined from four experimental geometries (taking into account that $\pi_{22} = \pi_{11}$) on the direct cut sample (see rows 1, 3, 5, 7) and from two experimental geometries on the sample of the $X/45°$-cut (rows 13 and 15). The other principal POCs π_{im} (i, m = 1, 2, 3), namely, $\pi_{12} = \pi_{21}$, $\pi_{13} = \pi_{23}$, $\pi_{31} = \pi_{32}$ and π_{33}, were determined from two experimental geometries. These POCs, defined from different experimental geometries, were the same in terms of the limits of the errors of their determination, thus proving the reliability of the obtained values. The mean-square values of POCs π_{im} calculated for different experimental geometries as well as their mean-square errors are indicated in the table showing the final results of the investigation of POE in lithium tantalate crystals (Table 4). For comparison, the data on the π_{im} coefficients for trigonal lithium niobate $LiNbO_3$ [27], calcium-tantalum gallosilicate $Ca_3TaGa_3Si_2O_{14}$ (CTGS) [4] and for lithium tantalate $LiTaO_3$, from the paper [37], are also shown in Table 4.
2. The non-principal POCs π_{14} and π_{24} were also determined from two independent experimental conditions (taking into account the equalities $\pi_{24} = -\pi_{14}$, $\pi_{42} = -\pi_{41}$, which are valid for the crystal class $3m$). Correspondingly, the mean-square values of these POCs and their mean-square errors are included in main results (Table 4).

Table 4. All independent piezo-optic coefficients π_{im} of $LiTaO_3$, $LiNbO_3$ and CTGS crystals (λ = 632.8 nm, T = 20 °C).

π_{im}, Br	π_{11}	π_{12}	π_{13}	π_{31}	π_{33}	π_{14}	π_{41}	π_{44}
$LiTaO_3$ (This Work)	−0.63 ± 0.05	0.47 ± 0.08	0.72 ± 0.10	0.54 ± 0.06	−0.27 ± 0.01	−0.43 ± 0.04	−0.29 ± 0.05	−0.06 ± 0.09
$LiTaO_3$ [37]	−0.62 ± 0.02	0.34 ± 0.03	0.64 ± 0.05	0.43 ± 0.02	−0.07 ± 0.01	0.40 ± 0.07	0.07 ± 0.03	0.41 ± 0.08
$LiNbO_3$ [27]	−0.38	+0.09	+0.80	+0.50	+0.20	−0.81	−0.88	+2.25
CTGS [4]	−0.19 ± 0.06	0.22 ± 0.09	0.53 ± 0.12	1.40 ± 0.19	−1.20 ± 0.09	0.72 ± 0.11	0.32 ± 0.11	−0.81 ± 0.40

Note: the value of POC π_{44} is lower than the error of its determination.

3. The errors of the determination of POCs π_{im} were calculated as mean-square values of the errors of two summands that were included in the expressions for the determination of POCs; specifically, the piezo-optic summand containing the control stresses σ^{o}_{im} and elastic summand formed by elastic compliance coefficient S_{km} or the combination of these coefficients. If the elastic component is formed by the sum of S_{km} coefficients (see, e.g., Equations (T. 2), (T. 5), (T. 8), etc.), the mean-square error of this sum should be determined. As can be seen in Table 1, the Equation (T. 10) for the determination of POC π_{44} includes sum of other POCs π_{im}. Therefore, before the calculation of the π_{44} coefficient, the mean-square error of the sum of the other POCs included in corresponding equation should be determined.
4. The comparison of sums of coefficients determined on the sample of the $X/45°$-cut (see, e.g., rows 16, 18, 21, etc. in Table 3) with the same sums of independent principal POCs defined on the direct cut sample shows that the results closely coincide with the limits of the error of their determination (Table 5). In particular, the value of the sum of POCs $\pi_{32} + \pi_{33} = 0.20 \pm 0.04$ Br. The same sum formed from independent

POCs $\pi_{31} = \pi_{32}$ and π_{33} (see Table 5) is equal to 0.27 ± 0.06 Br. Therefore, there is excellent agreement among the results. The analogous convergence of sums of POCs is also distinctive for other experimental geometries (see Table 5). On the one hand, this points to the reliability of the values of the principal POCs π_{im} and, on the other hand, to the objectivity of the results obtained on the sample of the $X/45°$-cut. Note that the sum of POCs $\pi_{12} + \pi_{13}$ obtained on the basis of the control stresses σ^o_{14} and $\sigma^o_{\overline{14}}$ coincides with the same sum of independent POCs. Based on the same control stresses, the π_{14} coefficient was determined, see formula (T. 7) in Table 1. Therefore, the value of π_{14} coefficient is also reliable. In the same way, the reliability of POC π_{41} can be proved. For this purpose, the formulae (T. 4), (T. 5) from Table 1 and the control stresses σ^o_{41}, $\sigma^o_{\overline{41}}$ (Table 3) have to be used.

5. Note the peculiarity of POE in the $LiTaO_3$ crystal. That is, the control stress $\sigma^o_{33} \to \infty$ (Table 3) for the experimental geometry m = 3, k = 1 (or k = 2), i = 3. This means that when applying uniaxial pressure along the $Z = X_3$ axis, the optical path does not change, i.e., the piezo-optic and elastic contributions to the optical path change $\delta\Delta_k$ are equal to the absolute values but opposite in terms of their signs. This can be shown on the basis of Expression (4), which describes the optical path change; under the experimental conditions m = 3, k = 1, i = 3. This expression can be written in the form

$$\frac{\delta\Delta_k}{\sigma_m d_k} = -\frac{1}{2}\pi_{im} n_i^3 + S_{km}(n_i - 1) \tag{16}$$

or, for the mentioned experimental conditions, one can obtain (in units, 10^{-12} m^2/N = 1 Br):

$$\begin{aligned} \frac{\delta\Delta_1}{\sigma_3 d_1} &= -\tfrac{1}{2}\pi_{33} n_3^3 + S_{13}(n_3 - 1) = -\tfrac{1}{2}(-0.27)\cdot 10.36 + (-1.17)\cdot(1.18) = \\ &= +1.400 - 1.381 = 0.02 \pm 0.16, \end{aligned} \tag{17}$$

where the error ± 0.16 is calculated as the mean-square value of the sum of errors of the first (piezo-optic) item of (17), i.e., 10% of the value of 1.400, and the second (elastic) item, i.e., 5% of the value of 1.381.

Therefore, the optical path change is an order lower that the error of its determination and two orders lower for each of the items in (17), i.e., $\delta\Delta_1/(\sigma_3 d_1) \to 0$.

Table 5. Sums of POCs obtained on the sample of the $X/45°$-cut ($LiTaO_3$ crystal).

No.	Experimental Conditions			$\Sigma\pi_{im}$ (Based on Direct Measurements), Br	$\Sigma\pi_{im}$ (Sum of Independent POCs), Br
	m	k	i		
1	1	$4(\bar{4})$	$\bar{4}(4)$	$\pi_{21} + \pi_{31} = 0.90 \pm 0.09$	1.01 ± 0.10
2	$4(\bar{4})$	1	2	$\pi_{22} + \pi_{23} = 0.14 \pm 0.04$	0.09 ± 0.11
3	$4(\bar{4})$	1	3	$\pi_{32} + \pi_{33} = 0.20 \pm 0.04$	0.27 ± 0.06
4	$4(\bar{4})$	$\bar{4}(4)$	1	$\pi_{12} + \pi_{13} = 1.04 \pm 0.12$	1.19 ± 0.13
5	$4(\bar{4})$	$\bar{4}(4)$	$4(\bar{4})$	$\pi_{24} + 2\pi_{42} = 0.99 \pm 0.09$	1.01 ± 0.09

6. For comparison, the POCs π_{im} for lithium niobate $LiNbO_3$ [27] and calcium-tantalum gallosilicate CTGS [4] are given in Table 4, which shows the main results for $LiTaO_3$. As can be seen in Table 4, the principal POCs of these crystals have the same signs (except for π_{33} coefficient of $LiNbO_3$). All principal POCs of lithium niobate and lithium tantalate crystals are relatively low (no higher than 1 Br). On the contrary, two coefficients (π_{31} and π_{33}) of the CTGS crystal are essentially higher than 1 Br.

From the comparison of the obtained values of POCs of π_{im} of $LiTaO_3$ crystal (first row in Table 4) with the data of [37] (second row), it follows that the essential discrepancies take place in the values of POCs π_{33}, π_{41}, π_{44} as well as in the signs of the non-principal POCs π_{14}, π_{41} and π_{44}. There are two factors that are clearly the reasons for these discrepancies: (1) the slight non-parallelism of the optical faces of a sample was not taken into account in [37], and this can be the source of considerable errors [19,27]; (2) the authors of [37] did not indicate how the positive directions of X, Y and Z axes of right coordinate system were chosen and, correspondingly, how the directions 4 and $\bar{4}$ were assigned on the sample of the $X/45°$-cut. Moreover, there were no data on the reliability of POC π_{im} in [37], whereas, in this paper, the reliability was proven by several results for different experimental geometries (see parts 1, 2 and 4 above). Because of considerable attention devoted to the reliability of the results in the present investigation, it can be argued that the obtained results of the study of POE in lithium tantalate are objective.

5. Elasto-Optic Coefficients of $LiTaO_3$ Crystals

ELOCs p_{in} were calculated on the basis of the tensor Expression (2), which is detailed in the following form for the 3m crystal class:

$$\begin{aligned} &p_{11} = \pi_{11}C_{11} + \pi_{12}C_{12} + \pi_{13}C_{13} + \pi_{14}C_{14}, p_{12} = \pi_{11}C_{12} + \pi_{12}C_{11} + \pi_{13}C_{13} - \pi_{14}C_{14}, \\ &p_{13} = (\pi_{11} + \pi_{12})C_{13} + \pi_{13}C_{33}, p_{31} = \pi_{31}(C_{11} + C_{12}) + \pi_{33}C_{13}, p_{33} = 2\pi_{31}C_{13} + \pi_{33}C_{33}, \\ &p_{14} = (\pi_{11} - \pi_{12})C_{14} + \pi_{14}C_{44}, p_{41} = \pi_{41}(C_{11} - C_{12}) + \pi_{44}C_{14}, p_{44} = 2\pi_{41}C_{14} + \pi_{44}C_{44}. \end{aligned} \quad (18)$$

POCs π_{im} from Table 4 (the first row) and elastic shiftiness coefficients C_{mk} from paper [35] (see Table 2, row 2) were used for the calculations. Their results are given in Table 6. In addition to the p_{in} values, the errors of their determination δp_{in} are also indicated in the Table. They were calculated as mean-square errors of the product $\pi_{im}{\cdot}C_{mk}$ based on the known expression $\delta(\pi_{im}{\cdot}C_{mk}) = [(\delta\pi_{im}{\cdot}C_{mk})^2 + (\pi_{im}{\cdot}\delta C_{mk})^2]^{1/2}$, which was used for each item in (18). For example, the following expression is valid for the determination of the error of the p_{13} coefficient:

$$\delta p_{13} = [(\delta\pi_{11}{\cdot}C_{13})^2 + (\delta\pi_{11}{\cdot}\delta C_{13})^2 + (\delta\pi_{12}{\cdot}C_{13})^2 + (\pi_{12}{\cdot}\delta C_{13})^2 + (\delta\pi_{13}{\cdot}C_{33})^2 + (\pi_{13}{\cdot}\delta C_{33})^2]^{1/2}. \quad (19)$$

Table 6. All independent elasto-optic p_{in} coefficients of $LiTaO_3$, $LiNbO_3$ and CTGS crystals (λ = 632.8 nm, T = 20 °C).

p_{im}	p_{11}	p_{12}	p_{13}	p_{31}	p_{33}	p_{14}	p_{41}	p_{44}
$LiTaO_3$ (This Work)	−0.076 ± 0.016	0.140 ± 0.021	0.191 ± 0.031	0.120 ± 0.016	0.003 * ± 0.008	−0.021 ± 0.006	−0.061 ± 0.013	0.009 * ± 0.011
$LiTaO_3$ [38]	−0.081 ± 0.003	0.081 ± 0.003	0.093 ± 0.02	0.089 ± 0.004	−0.044 ± 0.004	−0.026 ± 0.002	−0.085 ± 0.006	−0.028 ± 0.002
$LiNbO_3$ [39]	−0.021 ± 0.010	0.060 ± 0.012	0.172 ± 0.028	0.142 ± 0.018	0.118 ± 0.017	−0.052 ± 0.007	−0.109 ± 0.018	0.121 ± 0.033
$LiNbO_3$ [13]	−0.026	0.090	0.133	0.179	0.071	−0.075	−0.151	0.146
CTGS [4]	0.008 * ± 0.010	0.044 ± 0.013	0.096 ± 0.022	0.165 ± 0.031	−0.088 ± 0.031	0.029 ± 0.005	0.029 ± 0.015	0.033 ± 0.017

Note: the values of coefficients marked by asterisks (*) are lower than the errors of their determination.

The errors $\delta\pi_{im}$ are indicated for the values of π_{im} (Table 4), and the errors of the elastic shiftiness coefficients, represented by δC_{mk}, are calculated as 5% of the values of C_{mk} (in addition to the errors of the S_{km} coefficients). The important conclusion from the analysis of the contributions of items with errors $\delta\pi_{im}$ and δC_{mk} to the values of δp_{in} is that the main contributions are caused by errors of the piezo-optic coefficients, represented by $\delta\pi_{im}$. Namely, the contribution of $\delta\pi_{im}$ to δp_{11} is 87%, the contribution to δp_{12} is 95%, the contribution to δp_{13} is 94%, etc. Thus, a further conclusion that can be drawn is that a significant decrease in the ELOC error, represented by δp_{in}, requires a significant decrease in the POC error π_{im}. For this purpose, the precision of the experimental determination of the control stresses, $\sigma^{o}{}_{im}$, should be increased from 10% to (3–5%). This is a central problem that can be solved as needed.

It follows from the analysis of the results shown in Table 6 that the results for the p_{in} coefficients of the $LiNbO_3$ and $LiTaO_3$ crystals obtained by Avakyants and co-authors [13,38] (the Brillouin scattering method) are in good agreement with our data on lithium niobate [39]. In particular, the deviation of the values of the p_{11} coefficient obtained in [13] and [39] from their average value is small, and this deviation is equal to 10.5%. Thus, we found good convergence of the results obtained by means of the static interferometric technique [39] and the dynamic (acousto-optic) method of Brillouin scattering [13]. Unfortunately, such a convergence was not observed in the case of lithium tantalate [38]. It can be assumed that the convergence of our results with the ones of [38] would be better if all parameters (π_{im}, p_{in}, S_{km}, C_{mk}) are measured on the same samples and, moreover, if the thermodynamic (electrical) conditions of these measurements (with a constant electric field or induction, E = const or D = const) are taken into consideration.

As can also be seen in Table 6, the trigonal $LiTaO_3$, $LiNbO_3$ and CTGS crystals reveal a slight overall elasto-optic effect. The maximal values of the ELOCs p_{in} of these crystals are commensurate and are not higher than 0.191 for $LiTaO_3$, 0.179 for $LiNbO_3$ and 0.165 for CTGS. However, the positive characteristics of these crystals—namely high mechanical strength, high optical quality and resistance to aggressive environments—as well as the existence of effective technologies for the growth of large single crystals make these crystals the most important objects in applications related to photo-elastic or acousto-optic devices for the purpose of optical beam control. Maximal elasto-optic or acousto-optic efficiencies of these crystals can be determined from the analysis of surfaces that are indicative of the above-mentioned effect to varying degrees, see, e.g., papers [40–45] and others.

6. Conclusions

The piezo-optic effect in trigonal $LiTaO_3$ crystals was investigated through the use of the interferometric method. The experiment was carried out for the maximal number of possible experimental geometries in order to demonstrate the reliability (objectivity) of the results. In particular, the principal piezo-optic coefficient (POC) π_{11} was determined from six experimental geometries, and all other principal POCs π_{im} (i, m = 1, 2, 3) as well as non-principal POCs π_{14}, π_{41}, π_{44} were determined from two experimental geometries. The convergence of sums of independent POCs, such as $\pi_{12} + \pi_{13}$ and others, obtained for the samples of the $X/45^{\circ}$ cut with the ones obtained for the direct cut samples was shown. Our approach makes it possible to prove the reliability of the obtained data and the piezo-optical identity of the samples cut from the different parts of crystal boule, or those from different boules.

The main results of the work are the following:

1. All relationships for complex experimental geometries were obtained for the crystals of the 32, $3m$ and $\overline{3}m$ symmetry classes.
2. The ambiguity of the determination of problematic POCs π_{14}, π_{41} was eliminated, in terms of both the sign and the absolute value, through the unambiguous selection of the correct coordinate system. The condition $S_{14} > 0$ (S_{14} is the elastic compliance coefficient) was used for this purpose.
3. The effect non-typical for $LiTaO_3$ crystals was revealed: with the application of uniaxial pressure along the Z axis, the change of the optical path of a light beam $\delta\Delta_k \to 0$.
4. All independent components of the matrix of elasto-optic coefficients, represented by p_{in}, were calculated based on the components of the POCs matrix, π_{im}, which were determined by means of the interferometric technique. The comparative analysis of the p_{in} coefficients of $LiTaO_3$ and $LiNbO_3$, which were determined through the static interferometric method and the dynamic (acousto-optic) Brillouin scattering method, was carried out.
5. The $LiTaO_3$ crystals, as well as the $LiNbO_3$ [27,39] and $Ca_3TaGa_3Si_2O_{14}$ [4] crystals that were previously investigated by us, revealed relatively low elasto-optic effect (the maximal value of ELOC was $p_{in} \approx 0.2$). However, their high mechanical strength, high optical quality and resistance to aggressive environments, as well as the availability of effective technologies for the growth of large single crystals, were found to be excellent baselines for applications that make use of these crystals.

Author Contributions: Conceptualization, B.M.; Data curation, B.M. and N.D.; Investigation, B.M., N.D. and A.A.; Methodology, B.M., N.D. and A.A.; Resources, N.D. and O.B.; Writing—original draft, O.B.; Writing—review and editing, B.M. and O.B. All authors have read and agreed to the published version of the manuscript.

Funding: This work was supported by the National Research Foundation of Ukraine (Project 2020.02/0211) and The Ministry of Education and Science of Ukraine (project 0120U102204, DB/OPTYMA). Furthermore, the work was partially supported by the European Union's Horizon 2020 research and innovation program under the Marie Skłodowska-Curie grant agreement No. 778156.

Conflicts of Interest: The authors declare no conflict of interest.

References

1. Nye, J.F. *Physical Properties of Crystals*; Clarendon Press: Oxford, UK, 1964.
2. Narasimhamurty, T.S. *Photoelastic and Electrooptic Properties of Crystals*; Plenum Press: New York, NY, USA, 1981.
3. Mytsyk, B. Methods for the studies of the piezo-optical effect in crystals and the analysis of experimental data. I. Methodology for the studies of piezo-optical effect. *Ukr. J. Phys. Opt.* **2003**, *4*, 1–26.
4. Mytsyk, B.; Suhak, Y.; Demyanyshyn, N.; Buryy, O.; Syvorotka, N.; Sugak, D.; Ubizskii, S.; Fritze, H. Full set of piezo-optic and elasto-optic coefficients of $Ca_3TaGa_3Si_2O_{14}$ crystals at room temperature. *Appl. Opt.* **2020**, *59*, 8951–89585. [CrossRef]
5. Dixon, R.W.; Cohen, M.G. A new technique for measuring magnitudes of photoelastic tensors and its application to lithium niobate. *Appl. Phys. Lett.* **1966**, *8*, 205–207. [CrossRef]
6. Dixon, R.W. Photoelastic properties of selected materials and their relevance for applications to acoustic light modulators and scanners. *J. Appl. Phys.* **1967**, *38*, 5149–5153. [CrossRef]
7. Bergmann, L. *Der Ultraschall*; S. Hirzel Verlag: Leipzig, Germany, 1954.
8. Pettersen, H.E. New ultrasonic technique for the determination of the ratios of strain-optical constants. *J. Acoust. Soc. Am.* **1970**, *48*, 1093–1097. [CrossRef]
9. Narasimhamurty, T.S. Ultrasonic methods of determining elasto-optic constants of uniaxial and biaxial crystals. *Acta Crystallogr.* **1961**, *14*, 1176–1179. [CrossRef]
10. Yamada, M.; Wasa, K.; Hamaguchi, C. Brillouin scattering in GaP. *Jap. J. Appl. Phys.* **1976**, *15*, 1107–1111. [CrossRef]
11. Azuhata, T.; Takesada, M.; Yagi, T.; Shikanai, A.; Chichibu, S.F.; Torii, K.; Nakamura, A.; Sota, T.; Cantwell, G.; Eason, D.B.; et al. Brillouin scattering study of ZnO. *J. Appl. Phys.* **2003**, *94*, 968–972. [CrossRef]
12. Trzaskowska, A.; Mielcarek, S.; Mroz, B.; Trybula, Z. Elastic and elasto-optical properties of $Rb_{1-x}(NH_4)_xH_2AsO_4$ mixed crystals studied by Brillouin spectroscopy. *Cryst. Res. Technol.* **2010**, *45*, 48–52. [CrossRef]
13. Avakyants, L.P.; Kiselev, D.F.; Shchitov, N.N. Photoelasticity of $LiNbO_3$. *Fiz. Tverd. Tela* **1976**, *18*, 1547–1551.
14. Avakyants, L.P.; Antipov, V.V.; Kiselev, D.F.; Sorokin, N.G.; Zakutailov, K.V. Acoustooptic parameters of calcium molybdate crystals. *Fiz. Tverd. Tela* **1982**, *24*, 3171–3172.
15. Shaskol'skaya, M.P. *Acoustic Crystals. A Handbook*; Nauka: Moscow, 1982.
16. Mytsyk, B.H. *Photoelasticity of Anisotropic Materials*; Liga-Press: Lviv, Ukraine, 2012.
17. Narasimhamurty, T.S. Photoelastic behavior of rochelle salt. *Phys. Rev.* **1969**, *186*, 945–948. [CrossRef]
18. Shahabuddin, M.K.; Narasimhamurty, T.S. Photoelastic studies on ammonium Rochelle salt single crystal. *Sol. State Communic.* **1982**, *43*, 941–943. [CrossRef]
19. Mytsyk, B.; Demyanyshyn, N.; Martynyuk-Lototska, I.; Vlokh, R. Piezo-optic, photoelastic and acousto-optic properties of SrB_4O_7 crystals. *Appl. Opt.* **2011**, *50*, 3889–3895. [CrossRef]
20. Mytsyk, B.G.; Andrushchak, A.S.; Kost', Y.P. Static photoelasticity of gallium phosphide crystals. *Crystallogr. Rep.* **2012**, *57*, 124–130. [CrossRef]
21. Mytsyk, B.G.; Andrushchak, A.S.; Vynnyk, D.M.; Demyanyshyn, N.M.; Kost', Y.P.; Kityk, A.V. Characterization of photoelastic materials by combined Mach-Zehnder and conoscopic interferometry: Application to tetragonal lithium tetraborate crystals. *Opt. Laser. Eng.* **2020**, *127*, 105991/1−8. [CrossRef]
22. Mytsyk, B.G.; Kost', Y.P.; Demyanyshyn, N.M.; Andrushchak, A.S.; Solskii, I.M. Piezo-optic coefficients of $CaWO_4$ crystals. *Crystallogr. Rep.* **2015**, *60*, 130–137. [CrossRef]
23. Krupych, O.; Savaryn, V.; Vlokh, R. Precise determination of full matrix of piezo-optic coefficients with a four-point bending technique: The example of lithium niobate crystals. *Appl. Opt.* **2014**, *53*, B1–B7. [CrossRef] [PubMed]
24. Stadnyk, V.Y.; Brezvin, R.S.; Rudysh, M.Y.; Shchepanskii, P.A.; Kurlyak, V.Y. Piezo-optic properties of $LiNH_4SO_4$ crystals. *Crystallogr. Rep.* **2015**, *60*, 388–392. [CrossRef]
25. Stadnyk, V.J.; Romanyuk, M.O. Piezooptic properties of $(NH_4)_2BeF_4$ crystals. *Phys. Stat. Sol. A.* **1996**, *158*, 289–296.
26. Mytsyk, B.G.; Demyanyshyn, N.M.; Andrushchak, A.S.; Kost', Y.P.; Parasyuk, O.V.; Kityk, A.V. Piezooptical coefficients of $La_3Ga_5SiO_{14}$ and $CaWO_4$ crystals: A combined optical interferometry and polarization-optical study. *Opt. Mater.* **2010**, *33*, 26–30. [CrossRef]
27. Mytsyk, B.G.; Andrushchak, A.S.; Demyanyshyn, N.M.; Kost', Y.P.; Kityk, A.V.; Mandracci, P.; Schranz, W. Piezo-optic coefficients of MgO-doped $LiNbO_3$ crystals. *Appl. Opt.* **2009**, *48*, 1904–1911. [CrossRef] [PubMed]
28. Montalto, L.; Paone, N.; Scalise, L.; Rinaldi, D. A photoelastic measurement system for residual stress analysis in scintillating crystals by conoscopic imaging. *Rev. Sci. Instrum.* **2015**, *86*, 063102. [CrossRef]
29. Montalto, L.; Paone, N.; Rinaldi, D.; Scalise, L. Inspection of birefringent media by photoelasticity: From diffuse light polariscope to laser conoscopic technique. *Opt. Eng.* **2015**, *54*, 081210. [CrossRef]
30. Montalto, L.; Natali, P.P.; Scalise, L.; Paone, N.; Davì, F.; Rinaldi, D.; Barucca, G.; Mengucci, P. Quality control and structural assessment of anisotropic scintillating crystals. *Crystals* **2019**, *9*, 376. [CrossRef]
31. Rinaldi, D.; Montalto, L.; Natali, P.P.; Davì, F. Elasto-optic properties and internal stress analysis for monoclinic and trigonal crystals. *J. Instrum.* **2021**, *16*, P08018. [CrossRef]
32. Mytsyk, B.G.; Kost', Y.P.; Demyanyshyn, N.M.; Gaba, V.M.; Sakharuk, O.M. Study of piezo-optic effect of calcium tungstate crystals by the conoscopic method. *Opt. Mater.* **2015**, *39*, 69–73. [CrossRef]

33. Mytsyk, B.G.; Demyanyshyn, N.M.; Solskii, I.M.; Sakharuk, O.M. Piezo- and elasto-optic coefficients for calcium tungstate crystals. *Appl. Opt.* **2016**, *55*, 9160–9165. [CrossRef]
34. Warner, A.W.; Onoe, M.; Coquin, G.A. Determination of elastic and piezoelectric constants for crystals in class (3*m*). *J. Acoust. Soc. Am.* **1967**, *42*, 1223–1231. [CrossRef]
35. Yamada, T.; Iwasaki, H.; Niizeki, N. Piezoelectric and elastic properties of $LiTaO_3$: Temperature characteristics. *Jap. J. Appl. Phys.* **1969**, *8*, 1127–1132. [CrossRef]
36. Takanaga, I.; Kushibiki, J. Elastic constants of multidomain $LiTaO_3$ crystal. *J. Appl. Phys.* **1999**, *86*, 3342–3346. [CrossRef]
37. Mytsyk, B.G.; Andrushchak, A.S.; Pryriz, Y.V. Piezo-optic effect in lithium tantalate crystals. *Ukr. J. Phys.* **1992**, *37*, 1239–1244.
38. Avakyants, L.P.; Kiselev, D.F.; Shchitov, N.N. Photo-elastic constants of $LiTaO_3$. *Fiz. Tverd. Tela.* **1976**, *18*, 2129–2130.
39. Mytsyk, B.H.; Demyanyshyn, N.M.; Kost, Y.P. Signs of elastooptical coefficients in low-symmetry materials. *Mater. Sci.* **2015**, *50*, 762–770. [CrossRef]
40. Buryy, O.; Andrushchak, N.; Ratych, A.; Demyanyshyn, N.; Mytsyk, B.; Andrushchak, A. Global maxima for the acousto-optic effect in SrB_4O_7 crystals. *Appl. Opt.* **2017**, *56*, 1839–1845.
41. Buryy, O.; Demyanyshyn, N.; Mytsyk, B.; Andrushchak, A. Optimizing of the piezo-optic interaction geometry in SrB_4O_7 crystals. *Opt. Appl.* **2016**, *46*, 447–459.
42. Mys, O.; Kostyrko, M.; Krupych, O.; Vlokh, R. Anisotropy of the acoustooptic figure of merit for $LiNbO_3$ crystals. Isotropic diffraction. *App. Opt.* **2015**, *54*, 8176–8186. [CrossRef]
43. Mys, O.; Krupych, O.; Vlokh, R. Anisotropy of an acoustooptic figure of merit for KH_2PO_4 crystals. *Ukr. J. Phys. Opt.* **2017**, *18*, 83–94. [CrossRef]
44. Kupreychik, M.I.; Balakshy, V.I. Peculiarities of acousto-optic interaction biaxial crystal of alpha-iodic acid. *Appl. Opt.* **2018**, *57*, 5549–5555. [CrossRef] [PubMed]
45. Nikitin, P.A. Method for calculating the maximum value of the acousto-optic figures of merit of optically isotropic media. *Bull. Russ. Acad. Sci. Physics.* **2017**, *81*, 84–88. [CrossRef]